Microbiology (2013), **159**, 2674–2689 **DOI** 10.1099/mic.0.071340-0

Kinetic modelling of the *Zymomonas mobilis* Entner–Doudoroff pathway: insights into control and functionality

Reinis Rutkis,[1] Uldis Kalnenieks,[1] Egils Stalidzans[2] and David A. Fell[3]

Correspondence
Reinis Rutkis
reinisrutkis@gmail.com

[1]Institute of Microbiology and Biotechnology, University of Latvia, Kronvalda Boulv. 4, Riga LV-1586, Latvia

[2]Biosystems Group, Department of Computer Systems, Latvia University of Agriculture, Liela Iela 2, Jelgava LV-3001, Latvia

[3]Department of Biological and Medical Sciences, Oxford Brookes University, Headington, Oxford OX3 0BP, UK

Received 16 July 2013
Accepted 30 September 2013

Zymomonas mobilis, an ethanol-producing bacterium, possesses the Entner–Doudoroff (E-D) pathway, pyruvate decarboxylase and two alcohol dehydrogenase isoenzymes for the fermentative production of ethanol and carbon dioxide from glucose. Using available kinetic parameters, we have developed a kinetic model that incorporates the enzymic reactions of the E-D pathway, both alcohol dehydrogenases, transport reactions and reactions related to ATP metabolism. After optimizing the reaction parameters within likely physiological limits, the resulting kinetic model was capable of simulating glycolysis *in vivo* and in cell-free extracts with good agreement with the fluxes and steady-state intermediate concentrations reported in previous experimental studies. In addition, the model is shown to be consistent with experimental results for the coupled response of ATP concentration and glycolytic flux to ATPase inhibition. Metabolic control analysis of the model revealed that the majority of flux control resides not inside, but outside the E-D pathway itself, predominantly in ATP consumption, demonstrating why past attempts to increase the glycolytic flux through overexpression of glycolytic enzymes have been unsuccessful. Co-response analysis indicates how homeostasis of ATP concentrations starts to deteriorate markedly at the highest glycolytic rates. This kinetic model has potential for application in *Z. mobilis* metabolic engineering and, since there are currently no E-D pathway models available in public databases, it can serve as a basis for the development of models for other micro-organisms possessing this type of glycolytic pathway.

INTRODUCTION

Zymomonas mobilis is a facultatively anaerobic, ethanol-producing bacterium that possesses the Entner–Doudoroff (E-D) pathway, which differs in several respects from glycolysis and the pentose phosphate pathway typical of other organisms. The intrinsically rapid carbohydrate metabolism of *Z. mobilis* has been studied in great detail during the past decades (Barrow *et al.*, 1984; Osman *et al.*, 1987; De Graaf *et al.*, 1999) and all the enzymes of the E-D pathway have been purified and characterized kinetically (Scopes, 1983, 1984, 1985; Scopes *et al.*, 1985; Scopes & Griffiths Smith, 1984, 1986; Kinoshita *et al.*, 1985; Pawluk *et al.*, 1986). Complete genome sequences for various *Z. mobilis* strains have been reported in recent years, providing the opportunity to compare currently uncharacterized *Z. mobilis* enzymes with those from different databases (Seo *et al.*, 2005; Kouvelis *et al.*, 2009; Pappas *et al.*, 2011; Desiniotis *et al.*, 2012). In spite of these diverse studies, this accumulated knowledge has scarcely yet been exploited as the basis for building a comprehensive kinetic model of this key component of *Z. mobilis* central metabolism. The only recent attempt focused on the aspects of interaction between the engineered non-oxidative part of the pentose phosphate pathway and the native *Z. mobilis* E-D glycolysis for xylose fermentation,

Abbreviations: ADH, alcohol dehydrogenase; AK, adenylate kinase; E-D pathway, Entner–Doudoroff pathway; ENO, enolase; GAPD, glyceraldehyde-3-phosphate dehydrogenase; GF, glucose facilitator; GK, glucokinase; GPD, glucose-6-phosphate dehydrogenase; KDPGA, 2-keto-3-deoxy-6-phosphogluconate aldolase; MCA, metabolic control analysis; PDC, pyruvate decarboxylase; PEP, phosphoenolpyruvate; PGD, 6-phosphogluconate dehydratase; PGK, 3-phosphoglycerate kinase; PGL, 6-phosphogluconolactonase; PGM, phosphoglycerate mutase; PYK, pyruvate kinase.

Supplementary material is available with the online version of this paper.

assuming constant intracellular concentrations of the essential metabolic cofactors ADP, ATP, NAD(P)$^+$ and NAD(P)H (Altintas *et al.*, 2006). Whilst such a simplification certainly reduces model complexity, since the E-D pathway itself is a major component of ATP and NAD(P)(H) turnover, this assumption of their constant concentrations significantly limits applicability of the model. In order to investigate interactions between the various ATP consumption reactions and the E-D pathway, a generalized ATP-consuming reaction has been introduced into the E-D

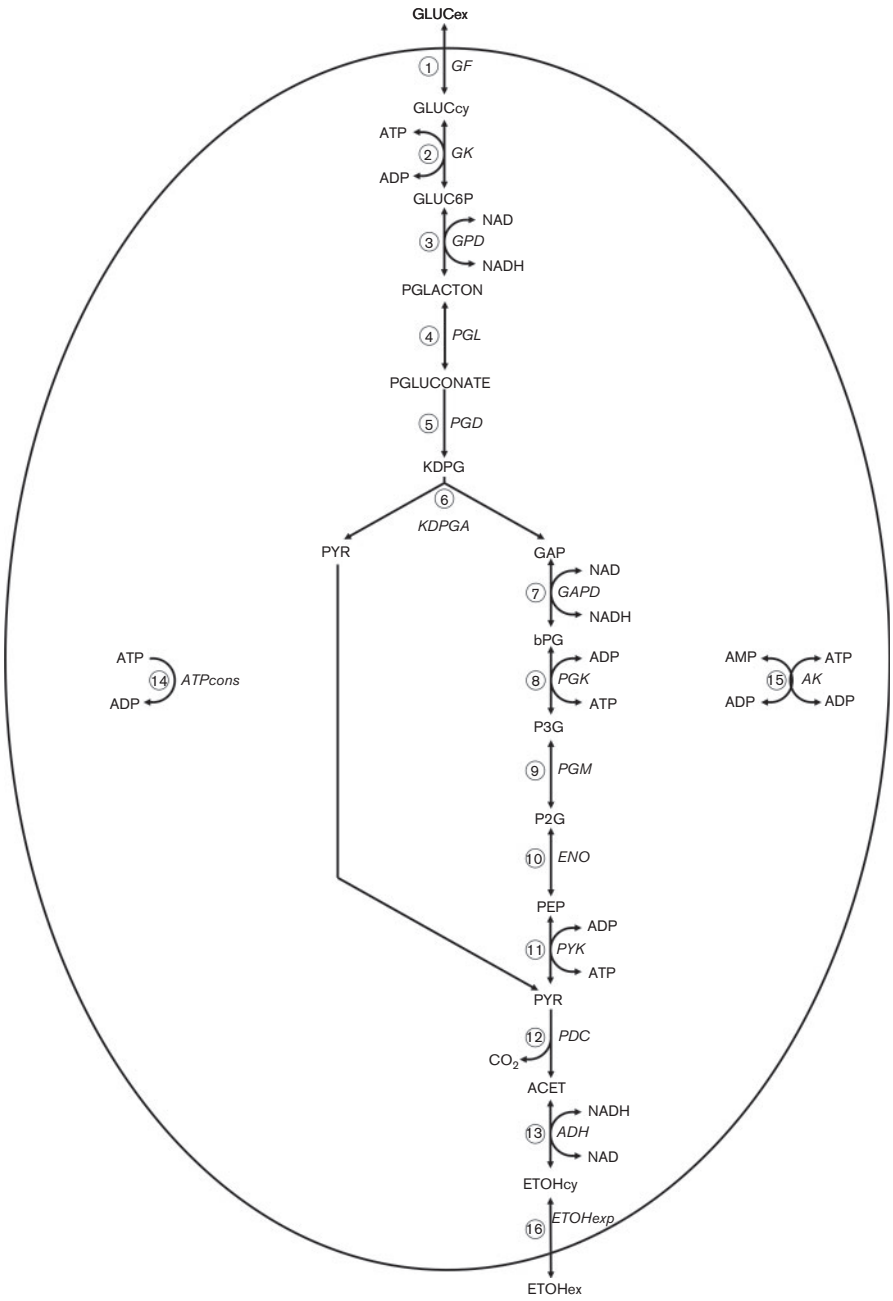

Fig. 1. Reactions included in the model of the E-D glucose utilization pathway. The numbered enzymes in these pathways are: (1) glucose facilitator (GF); (2) glucokinase (GK); (3) glucose-6-phosphate dehydrogenase (GPD); (4) 6-phosphogluconolactonase (PGL); (5) 6-phosphogluconate dehydratase (PGD); (6) 2-keto-3-deoxy-6-phosphogluconate aldolase (KDPGA); (7) glyceraldehyde-3-phosphate dehydrogenase (GAPD); (8) 3-phosphoglycerate kinase (PGK); (9) phosphoglycerate mutase (PGM); (10) enolase (ENO); (11) pyruvate kinase (PYK); (12) pyruvate decarboxylase (PDC); (13) alcohol dehydrogenase (ADH); (14) ATP-consuming reactions (ATPcons); (15) adenylate kinase (AK); (16) ethanol export (ETOHexp). Other abbreviations are defined in Table S1.

Table 1. Rate equations used in this study

The reaction numbers correspond to those depicted in Fig. 1.

No.	Reaction	Rate equation
1	$v_{GF}=$	$\dfrac{\frac{V_f}{K_{mGLUCex}}*\left(GLUC_{ex}-\frac{GLUC_{cy}}{K_{eq}}\right)}{1+\frac{GLUC_{ex}}{K_{mGLUCex}}+\frac{GLUC_{cy}}{K_{mGLUCcy}}}$
2	$v_{GK}=$	$\dfrac{\frac{V_f}{K_{mGLUCcy}*K_{mATP}*\left(1+\frac{GLUC6P}{K_{iGLUC6P}}\right)}*\left(GLUC_{cy}*ATP-\frac{GLUC6P*ADP}{K_{eq}}\right)}{1+\frac{GLUC_{cy}}{K_{mGLUCcy}}+\frac{GLUC6P}{K_{mGLUC6P}}*\left(1+\frac{ATP}{K_{mATP}*\left(1+\frac{GLUC6P}{K_{iGLUC6P}}\right)}+\frac{ADP}{K_{mADP}}\right)}$
3	$v_{GPD}=$	$\dfrac{V_f*\frac{GLUC6P}{K_{mGLUC6P}}*\frac{NAD}{K_{mNAD}*\left(1+\frac{ATP}{K_{mATP}}\right)}*\left(1-\frac{PGLACTON*NADH}{GLUC6P*NAD*K_{eq}}\right)*}{\left(\frac{1+\left(\frac{PEP}{K_{iPEP}}\right)^b}{1+\sigma^{4b}\left(\frac{PEP}{K_{iPEP}}\right)^b}+\frac{1+\sigma^{2b}\left(\frac{PEP}{K_{iPEP}}\right)^b}{1+\sigma^{4b}\left(\frac{PEP}{K_{iPEP}}\right)^b}\right)*\left\{\left(\frac{GLUC6P}{K_{mGLUC6P}}+\frac{PGLACTON}{K_{mPGLACTON}}\right)^b+\left(\frac{GLUC6P}{K_{mGLUC6P}}+\frac{PGLACTON}{K_{mPGLACTON}}\right)^{b-1}*\left(\frac{NAD}{K_{mNAD}*\left(1+\frac{ATP}{K_{mATP}}\right)}+\frac{NADH}{K_{mNADH}}\right)^{b-1}\right\}*\left(\frac{NAD}{K_{mNAD}*\left(1+\frac{ATP}{K_{mATP}}\right)}+\frac{NADH}{K_{mNADH}}\right)^b+\left(\frac{GLUC6P}{K_{mGLUC6P}}+\frac{PGLACTON}{K_{mPGLACTON}}\right)^b*\left(\frac{NAD}{K_{mNAD}*\left(1+\frac{ATP}{K_{mATP}}\right)}+\frac{NADH}{K_{mNADH}}\right)^b}$
4	$v_{PGL}=$	$\dfrac{\frac{V_f}{K_{mPGLACTON}*\left(1+\frac{GLUC6P}{K_{iGLUC6P}}\right)}*\left(PGLACTON-\frac{PGLUCONATE}{K_{eq}}\right)}{1+\frac{PGLACTON}{K_{mPGLACTON}*\left(1+\frac{GLUC6P}{K_{iGLUC6P}}\right)}+\frac{PGLUCONATE}{K_{mPGLUCONAT}}}$
5	$v_{PGD}=$	$\dfrac{V_f*\frac{PGLUCONATE}{K_{mPGLUCONATE}*\left(1+\frac{P3G}{K_{iP3G}}\right)}}{1+\frac{PGLUCONATE}{K_{mPGLUCONATE}*\left(1+\frac{P3G}{K_{iP3G}}\right)}}$
6	$v_{KDPGA}=$	$\dfrac{\frac{V_f*KDPG}{K_{mKDPG}}-\frac{V_f*GAP*PYR}{K_{eq}*K_{mKDPG}}}{1+\frac{KDPG}{K_{mKDPG}}+\frac{PYR}{K_{mPYR}}+\frac{GAP}{K_{mGAP}}+\frac{KDPG*GAP}{K_{mKDPG}*K_{iGAP}}+\frac{PYR*GAP}{K_{mPYR}*K_{mGAP}}}$
7	$v_{GAPD}=$	$\dfrac{\frac{V_f}{K_{mGAP}*K_{mNAD}}*\left(GAP*NAD-\frac{bPG*NADH}{K_{eq}}\right)}{\left(1+\frac{GAP}{K_{mGAP}}+\frac{bPG}{K_{mbPG}}\right)*\left(1+\frac{NAD}{K_{mNAD}}+\frac{NADH}{K_{mNADH}}\right)}$
8	$v_{PGK}=$	$\dfrac{\frac{V_f}{K_{mbPG}*K_{mADP}}*\left(bPG*ADP-\frac{P3G*ATP}{K_{eq}}\right)}{\left(1+\frac{bPG}{K_{mbPG}}+\frac{P3G}{K_{mP3G}}\right)*\left(1+\frac{ADP}{K_{mADP}}+\frac{ATP}{K_{mATP}}\right)}$

Table 1. cont.

No.	Reaction	Rate equation
9	$v_{PGM}=$	$\frac{\frac{V_f}{K_{mP3G}}*\left(P3G-\frac{P2G}{K_{eq}}\right)}{1+\frac{P3G}{K_{mP3G}}+\frac{P2G}{K_{mP2G}}}$
10	$v_{ENO}=$	$\frac{\frac{V_f}{K_{mP2G}}*\left(P2G-\frac{PEP}{K_{eq}}\right)}{1+\frac{P2G}{K_{mP2G}}+\frac{PEP}{K_{mPEP}}}$
11	$v_{PYK}=$	$\frac{\frac{V_f}{K_{mPEP}*K_{mADP}}*\left(PEP*ADP-\frac{PYR*ATP}{K_{eq}}\right)}{\left(1+\frac{PEP}{K_{mPEP}}+\frac{PYR}{K_{mPYR}}\right)*\left(1+\frac{ADP}{K_{mADP}}+\frac{ATP}{K_{mATP}}\right)}$
12	$v_{PDC}=$	$\frac{V_f*\frac{PYR}{K_{mPYR}}}{1+\frac{PYR}{K_{mPYR}}}$
13	$v_{ADH}=$	$\frac{\frac{V_f*NADH*ACET}{K_{iNADH}*K_{mACET}}-\frac{V_f*K_{mNAD}*NAD*ETOH}{K_{eq}*K_{mNADH}*K_{mACET}*K_{iNAD}}}{1+\frac{NADH}{K_{iNADH}}+\frac{K_{mNADH}*ACET}{K_{iNADH}*K_{mACET}}+\frac{NADH*ACET}{K_{iNADH}*K_{mACET}}+\frac{NAD}{K_{iNAD}}+\frac{K_{mNAD}*ETOH}{K_{mETOH}*K_{iNAD}}+\frac{ETOH*NAD}{K_{mETOH}*K_{iNAD}}}$
14	$v_{ATPCons}=$	$\frac{V_f*ATP}{K_{mATP}+ATP}$
15	$v_{AK}=$	$\frac{\frac{V_f}{K_{mADP}^2}*\left(ADP^2-\frac{ATP*AMP}{K_{eq}}\right)}{\left(1+\frac{ADP}{K_{mADP}}+\frac{ATP}{K_{mATP}}\right)*\left(1+\frac{ADP}{K_{mADP}}+\frac{AMP}{K_{mAMP}}\right)}$
16	$V_{ETOHexp}=$	$k*\left(ETOH_{cy}-ETOH_{ex}\right)$

model described here. It has previously been proposed that the constitutively high catabolic rate that makes *Z. mobilis* an outstanding ethanol producer must be complemented by an intrinsic growth-independent, ATP-wasting reaction. This latter might be responsible for the 'uncoupled growth' phenomenon in this bacterium (Jones & Doelle, 1991). Incorporating adenylate and nicotinamide nucleotide metabolism into a computer model also offers the potential to inform the debate about the details of the role of the organism's respiratory system in aerobic metabolism (Kalnenieks *et al.*, 1993, 2008; Strazdina *et al.*, 2012).

There is good reason to expect that kinetic modelling of the *Z. mobilis* E-D pathway could also find application in metabolic engineering of this bacterium. A recently published stoichiometric analysis of *Z. mobilis* central metabolism revealed several metabolic engineering strategies to obtain high-value products, such as glycerate, succinate and glutamate, and also suggested the possibility of glycerol conversion to ethanol (Pentjuss *et al.*, 2013). However, analysis of the stoichiometric matrix just uncovers these possibilities, and further in-depth studies of the dynamics and regulation of *Z. mobilis* central metabolism are required to proceed with metabolic engineering. Indeed, in spite of the recent progress in the molecular biology of *Z. mobilis*, attempts to optimize metabolic processes by overexpression of intuitively chosen enzymes that are thought to be important for the rate of ethanol formation have led to counterintuitive results, such as a decrease of glycolytic flux (Snoep *et al.*, 1995). Such reports underline the need for quantitative metabolic control analysis before selection of enzymes that might exert flux control in *Z. mobilis*; this can be directly achieved by means of kinetic modelling.

Currently, there are also no kinetic models of the E-D pathway in public databases for any other micro-organisms possessing this form of glycolysis. Therefore, our present attempt to use accumulated experimental knowledge for kinetic modelling of the *Z. mobilis* E-D pathway might be useful for broader applications in microbial metabolic engineering.

METHODS

Modelling

Characteristics of the system, simplifying assumptions and moiety conservation. The model includes all the enzymes of the E-D pathway, glucose facilitator (GF), alcohol dehydrogenases (ADHs) and a reaction simulating ethanol export (Fig. 1). As in other glycolytic models, we have lumped all ATP hydrolysing reactions into one general ATP-consuming reaction, whose initial properties are set according to experimental data, taking into account that the membrane-bound F_0F_1-type ATPase is responsible for a significant part of ATP turnover in *Z. mobilis* (Reyes & Scopes, 1991). We have added the adenylate kinase (AK) reaction to equilibrate the AMP, ADP and ATP pools according to experimental observations.

Glucose-6-phosphate dehydrogenase (GPD) of *Z. mobilis* acts on both NAD and NADP, but has a higher specific activity with the former (Scopes, 1997). Since both ADHs (Kinoshita *et al.*, 1985) are specific to NAD(H) rather than NADP(H), we assume that the E-D pathway is turning over NAD rather than NADP. Any activity of GPD with NADP is likely to be coupled with the biosynthetic demands of growth, but this represents only 2 % of the glucose consumption (Swings & De Ley, 1977; Rogers *et al.*, 1982).

Two moiety-conservation relationships can be computed from the stoichiometry matrix of this set of reactions: one attributable to adenine nucleotides and the other to the nicotinamide nucleotide pool. The moiety-conserved sum is assigned on the basis of experimental observations. According to earlier reports, the ATP content of the cell, depending on the growth medium used, is maintained between 900 and 3600 μM, and it remains constant during the exponential phase in the range 1200–1500 μM (Lazdunski & Belaich, 1972). These values are in good agreement with data obtained later, where maximal concentrations of AMP, ADP and ATP were estimated to be 1500–2000 μM, with the ATP/ADP ratio near 1, by the 18th hour of fermentation (Osman *et al.*, 1987). Therefore we have assumed the following total adenylate moiety:

$$ATP + ADP + AMP = 3500\ \mu M \quad (1)$$

Adenylate charge (Atkinson, 1968) is calculated as (ATP + ½ ADP)/3500 and is used for comparison of the adenine nucleotide status with experiments where the total adenylate concentration may have been different.

In the case of the nicotinamide conservation, we have assumed that NAD(H) makes up most of the 4500 μM intracellular NAD(P)(H) pool, detected in *Z. mobilis* by NMR, without taking into account NADP(H) (De Graaf *et al.* 1999). Hence:

$$NAD^+ + NADH = 4500\ \mu M \quad (2)$$

For steady state modelling, we maintained constant extracellular glucose and ethanol concentrations with respective values of 140 000 μM and 1000 μM. In time-course simulations, glucose and ethanol were variables of the model, simulated as a closed system.

Enzyme kinetics. The rate equations for the individual enzymic reactions are presented together with the transport reactions in Table 1. The numbers of these equations correspond with those depicted in Fig. 1. All the equations were modelled according to the available literature data on *Z. mobilis* enzyme kinetics using generic, reversible rate equations (see Appendix), with the exception of GPD, where we directly fitted experimental observations (Scopes, 1997) to the universal rate equation for systems biology (Rohwer *et al.*, 2007). The source of the initial parameter values and more detailed derivations of the enzymic rate equations are given in the supplementary material (available in *Microbiology* Online). Enzyme rate units were all converted to micromoles per second per litre cell volume (μmol l^{-1} s^{-1}).

The model was built by entering these rate equations into the COPASI biochemical simulation software package, v. 4.8 (Hoops *et al.*, 2006), which assembles the set of ordinary differential equations automatically.

Glucose uptake fluxes in micromoles per second reported by COPASI were converted to grams of glucose per gram dry weight per hour (g g^{-1} h^{-1}) for comparison with experimentally reported measurements. For calculations we assumed that 1 mg dry weight of biomass corresponds to 2.2 μl of intracellular volume on average (Strohhäcker *et al.*, 1993).

Parameter optimization. Since the *in vitro* kinetic parameters were assembled from a variety of sources, in order to combine them into a coherent kinetic model, the maximum velocities of all reactions were optimized according to experimentally obtained steady-state intermediate concentrations. In order to have mutually compatible values for as many E-D intermediate concentrations as possible, and to avoid incompatibility of data coming from different analytical methods, we have used metabolite concentrations obtained by ^{31}P NMR in bacterial cells harvested at late exponential growth phase (Barrow *et al.*, 1984; Osman *et al.*, 1987). Metabolite concentrations were determined from spectra of extracts prepared 3–4 min after addition of glucose to cell suspensions, which correspond to quasi steady-state concentrations (Strohhäcker *et al.*, 1993). Initial values of the maximum velocities (V_f) were derived from the data of the 18th hour of batch fermentation (Osman *et al.*, 1987). This was chosen to ensure that the intermediate concentrations and V_f values used correspond roughly to the same physiological condition of the cells, where, according to ^{31}P NMR studies, specific glucose uptake rate slightly exceeds 5 g g^{-1} h^{-1} (De Graaf *et al.*, 1999), which we used as the target value of glycolytic flux for parameter optimization. This value is also in good agreement with earlier reports, where *Z. mobilis* was likewise grown in ^{31}P NMR experiments on 10 % glucose anaerobically (Rogers *et al.*, 1979).

According to previous reports, most of the enzymes from the E-D pathway change their activity up to fivefold during batch fermentation; therefore, the upper and lower boundaries of V_f values that we set for each reaction during parameter optimization was a factor of five above and below the initial value (Osman *et al.*, 1987). *K*m(i) values, which have been assumed or obtained from other databases attributable to other micro-organisms, were optimized within a factor of three above and below the initial value. Parameter optimization was also carried out using COPASI software using various optimization algorithms.

Quantifying the flux control. The control of a particular enzyme, *i*, on a glycolytic flux under steady-state conditions is defined by flux control coefficient C_i^J expressed as a percentage:

$$C_i^J = \frac{\partial J}{\partial v_i} * \frac{v_i}{J} * 100\% = \frac{\partial ln J}{\partial ln v_i} * 100\% \quad (3)$$

in which v_i is the rate of enzyme *i*, *J* is a steady-state pathway flux (Kacser & Burns, 1973; Fell, 1992). The flux control coefficients of enzymes and transporters were calculated by COPASI and the results obtained always obeyed the summation theorem (Kacser & Burns, 1973):

$$\sum_{i=1,\ldots n} C_i^J = 100\% \quad (4)$$

in which the summation is over all *n* enzymes in the model.

The effect of changing the activity (amount) of a single enzyme on the pathway flux was determined according to Small & Kacser (1993):

$$f = \frac{1}{1-\left[\frac{r-1}{r*100}\right]C_i^J} \quad (5)$$

in which f is the fold flux increase value and r is the fold increase of the enzyme activity.

Quantifying ATP homeostasis. Changes in an enzyme activity affect metabolite concentrations as well as fluxes and the concentration control coefficient quantifies the magnitude of this effect on a metabolite. It is defined in the same way as for the flux control coefficient. Thus, for metabolite S_j, the concentration control coefficient with respect to enzyme i is:

$$C_i^{S_j} = \frac{\partial S_j}{\partial v_i} * \frac{v_i}{S_j} * 100\,\% = \frac{\partial \ln S_j}{\partial \ln v_i} * 100\,\% \quad (6)$$

The extent to which metabolite concentrations can be maintained relatively constant as fluxes change is a measure of metabolic homeostasis (Hofmeyr *et al.*, 1993; Cornish-Bowden & Hofmeyr, 1994; Thomas & Fell, 1996, 1998). This can be quantified by the ratio of the metabolite's concentration control coefficient to the flux control coefficient of the same enzyme, which has been defined as the co-response coefficient (Hofmeyr *et al.*, 1993; Cornish-Bowden & Hofmeyr, 1994). Thus, for metabolite S_j, flux J and enzyme i as defined in equations 3 and 6:

$$\Omega_i^{S_j:J} = \frac{C_i^{S_j}}{C_i^J} = \frac{\partial \ln S_j}{\partial \ln J} \quad (7)$$

The final term in the above equation results from the terms $\partial \ln v_i$ and the scaling factor 100 cancelling from the equation. This is useful since it is not necessary to know the change in enzyme activity used to perturb the system in order to calculate the co-response coefficient from simultaneous measurements of metabolite concentration and flux, provided that the perturbation is produced by modulation of a single enzyme, *i*. This contrasts with experimental determinations of flux and concentration control coefficients, which do require a measure of the enzyme activity change involved. Hence the co-response coefficient may be obtained from the slope of a log–log graph of concentration against flux. Alternatively, for a small enough perturbation, the co-response coefficient may be approximated from the difference between adjacent points as:

$$\Omega_i^{S_j:J} \approx \frac{\Delta S_j}{\Delta J} \quad (8)$$

In this paper, we determine the ATP : $J_{glycolysis}$ co-response coefficient with respect to ATPase, i.e. $\Omega_{ATPase}^{ATP:Jglycolysis}$ in this way.

Experimental

Bacterial strains. Bacterial strains *Z. mobilis* ATCC 29191 (Zm6) and its mutant derivatives Zm6-*cytB* and Zm6-*cydB* used in the present study were maintained and cultivated as described previously (Strazdina *et al.*, 2012).

Preparation of non-growing cell suspensions. For the preparation of non-growing cell suspension, cells were harvested at late exponential phase, sedimented, washed and resuspended in 100 mM potassium phosphate buffer (pH 6.9), containing 2 mM magnesium sulfate, to a biomass concentration of 6.8–7.0 g (dry weight) l^{-1}.

Biochemical analyses. Samples for ATP determination were quenched in ice-cold 10 % trichloroacetic acid and assayed by the standard luciferin–luciferase method using an LKB Wallac 1251 Luminometer. Glucose concentration was measured by HPLC (Agilent 1100 series), using a Bio-Rad Aminex HPX–87H column.

RESULTS AND DISCUSSION

Initial model validation

In order to evaluate the model, the first question we addressed was whether the optimized E-D model is capable of reproducing glycolytic fluxes comparable to those reported earlier for *Z. mobilis*. The final version of our optimized model (hereafter – the optimized model) gave a specific glucose uptake rate of 4.9 g g^{-1} h^{-1}, close to our target. Evaluation of the difference between initial (Osman *et al.*, 1987) and optimized V_f values (Table 2) revealed that, for the majority of enzymes, these remained within a factor of three of the starting estimate and lie within the range of values reported across batch fermentation. V_f initial values used for parameter optimization for the majority of enzymes rose during optimization and came closer to values in French-press extracts reported earlier (Algar & Scopes, 1985). The calculated intermediate metabolite concentrations under steady conditions (Table 3), apart from phosphoenolpyruvate (PEP), were close to the NMR values within a factor of 1.5. The low PEP concentration predicted by the model is consistent with earlier reports that also suggest very low PEP intracellular levels (Algar & Scopes, 1985). Also the adenylate charge obtained (0.65) was consistent with experimental observations by Algar & Scopes (1985).

Simulation of glycolysis in cell-free extracts

To investigate whether the resulting model is able to simulate experiments other than those used for acquisition of initial parameters, we have carried out *in silico* simulation of earlier analyses of glycolysis in *Z. mobilis* (Algar & Scopes, 1985). First of all, by inserting reported E-D pathway enzyme activities in French-press extracts into the optimized model, we aimed to reproduce glycolysis *in situ*. Since Algar & Scopes did not report the activity for 6-phosphogluconolactonase, we have used our optimized value for this reaction. Also, phosphoglycerate kinase was assayed in the reverse direction and therefore the physiological activity for this reaction was calculated by using the Haldane relationship for multi-substrate reactions (Bisswanger, 2002). With these new enzyme activities, the model also reached steady state with a glycolytic flux in the model corresponding to an *in situ* rate of 5.2 g g^{-1} h^{-1}. This is in the range of the optimized model and earlier observations, where *Z. mobilis* was grown on different initial glucose concentrations with reported specific glucose uptake rates slightly below 5.5 g g^{-1} h^{-1} (Rogers *et al.*, 1979).

Table 2. Initial and optimized kinetic parameters of the model reactions

Units for each parameter are: V_f, μmol l^{-1} s^{-1}; K_m, K_i, μmol l^{-1}; k, 1 s^{-1}, Keq dimensionless, except reaction No.6, Keq, μmol.

No.	Reaction	Kinetic parameter	Value		Ratio	Reference
			Initial	Optimized	Optimized/initial	
1	Glucose facilitator (GF)	V_F	7000	7000	1.00	DiMarco & Romano (1985)
		K_{eq}	1			Assumed
		$K_{mGLUCex}$	5000			DiMarco & Romano (1985)
		$K_{mGLUCcy}$	5000			DiMarco & Romano (1985)
2	Glucokinase (GK)	V_F	6000	6263	1.04	Osman *et al.* (1987)
		K_{eq}	450			Robbins & Boyer (1957)
		$K_{mGLUCcy}$	220			Scopes *et al.* (1985)
		K_{mATP}	800			Scopes *et al.* (1985)
		$K_{iGLUC6P}$	15000			Scopes *et al.* (1985)
		$K_{mGLUC6P}$	1000	2608	2.61	Assumed
		K_{mADP}	1000	2458	2.46	Assumed
3	Glucose-6-phosphate dehydrogenase (GPD)	V_F	3500	17484	5.00	Osman *et al.* (1987)
		K_{eq}	1.4			Wurster *et al.* (1970), Glaser & Brown (1955)
		$K_{mGLUC6P}$	221.7			Calculated from Scopes (1997)
		K_{mNAD}	251.8			Calculated from Scopes (1997)
		$K_{mPGLACTON}$	1000	2994	2.99	Assumed
		K_{mATP}	1400			Scopes (1985)
		K_{mNADH}	1000	2998	3.00	Assumed
		K_{iPEP}	14.1			Calculated from Scopes (1997)
		h	1.75			Calculated from Scopes (1997)
		σ	0.5			Calculated from Scopes (1997)
4	Phosphogluconolactonase (PGL)	V_F	2000	7848	3.92	Osman *et al.* (1987)

Table 2. cont.

No.	Reaction	Kinetic parameter	Value		Ratio	Reference
			Initial	Optimized	Optimized/initial	
		K_{eq}	6400			Assumed from Goldberg *et al.* (2004)
		$K_{mPGLACTON}$	25			Scopes (1985)
		$K_{mPGLUCONATE}$	1000	351	0.35	Assumed
		$K_{iGLUC6P}$	300			Scopes (1985)
5	6-Phosphogluconate dehydratase (PGD)	V_F	2000	4925	2.46	Osman *et al.* (1987)
		$K_{mPGLUCONATE}$	50			Scopes & Griffiths-Smith (1984)
		K_{iP3G}	2000			Scopes & Griffiths-Smith (1984)
6	KDPG aldolase (KDPGA)	V_F	2000	7629	3.81	Osman *et al.* (1987)
		K_{eq}	1300			Assumed from Goldberg *et al.* (2004)
		K_{mKDPG}	250			Scopes (1984)
		K_{mPYR}	1000	2994	2.99	Assumed
		K_{mGAP}	1000	369	0.37	Assumed
		K_{iGAP}	1000	2996	3.00	Assumed
7	Glyceraldehyde-3-phosphate dehydrogenase (GAPD)	V_F	70000	53000	0.76	Osman *et al.* (1987)
		K_{eq}	0.04			Assumed from Goldberg *et al.* (2004)
		K_{mGAP}	210	292	1.39	Teusink *et al.* (2000)
		K_{mNAD}	90	133	1.48	Teusink *et al.* (2000)
		K_{mNADH}	60	107	1.78	Teusink *et al.* (2000)
		K_{mbPG}	10	9	0.90	Teusink *et al.* (2000)
8	3-Phosphoglycerate kinase (PGK)	V_F	9000	44990	5.00	Osman *et al.* (1987)
		K_{eq}	3000			Teusink *et al.* (2000), Krietsch & Bücher (1970)
		K_{mbPG}	3	5	1.50	Teusink *et al.* (2000)
		K_{mADP}	200	517	2.59	Teusink *et al.* (2000)
		K_{mP3G}	1500			Pawluk *et al.* (1986)
		K_{mATP}	1100			Pawluk *et al.* (1986)
9	Phosphoglycerate mutase (PGM)	V_F	45000	27454	0.61	Osman *et al.* (1987)

Table 2. cont.

No.	Reaction	Kinetic parameter	Value		Ratio	Reference
			Initial	Optimized	Optimized/initial	
		K_{eqPGM}	0.2			Teusink *et al.* (2000)
		K_{mP3G}	1100			Pawluk *et al.* (1986)
		K_{mP2G}	80	28	0.35	Teusink *et al.* (2000)
10	Enolase (ENO)	V_F	25000	5457	0.22	Osman *et al.* (1987)
		K_{eq}	4			Wold & Ballou (1957)
		K_{mP2G}	80			Pawluk *et al.* (1986)
		K_{mPEP}	500	167	0.33	Teusink *et al.* (2000)
11	Pyruvate kinase (PYK)	V_F	70000	88774	1.27	Osman *et al.* (1987)
		K_{eq}	5000			Assumed from Goldberg *et al.* (2004)
		K_{mPEP}	80			Pawluk *et al.* (1986)
		K_{mADP}	170			Pawluk *et al.* (1986)
		K_{mPYR}	210	78	0.37	Teusink *et al.* (2000)
		K_{mATP}	1500	502	0.33	Teusink *et al.* (2000)
12	Pyruvate decarboxylase (PDC)	V_F	7500	9731	1.30	Osman *et al.* (1987)
		K_{mPYR}	400			Bringer-Meyer *et al.* (1986)
13	Alcohol dehydrogenase (ADH I)	V_F	10000	2013	0.20	Kinoshita *et al.* (1985)
		K_{eq}	10000			Assumed from Goldberg *et al.* (2004)
		K_{mACET}	86			Kinoshita *et al.* (1985)
		K_{mNAD}	73			Kinoshita *et al.* (1985)
		K_{mNADH}	27			Kinoshita *et al.* (1985)
		K_{iNAD}	24			Kinoshita *et al.* (1985)
		K_{mETOH}	4800			Kinoshita *et al.* (1985)
		K_{iNADH}	7.6			Kinoshita *et al.* (1985)
13	Alcohol dehydrogenase (ADH II)	V_F	37500	184732	4.93	Kinoshita *et al.* (1985)

Table 2. cont.

No.	Reaction	Kinetic parameter	Value		Ratio	Reference
			Initial	Optimized	Optimized/initial	
		K_{eq}	10000			Assumed from Goldberg *et al.* (2004)
		K_{mACET}	1300			Kinoshita *et al.* (1985)
		K_{mNAD}	110			Kinoshita *et al.* (1985)
		K_{mNADH}	12			Kinoshita *et al.* (1985)
		K_{iNAD}	140			Kinoshita *et al.* (1985)
		K_{mETOH}	27000			Kinoshita *et al.* (1985)
		K_{iNADH}	18			Kinoshita *et al.* (1985)
14	ATP consumption (ATPcons)	V_F	6000	4428	0.74	Reyes & Scopes (1991)
		K_{mATP}	500			Reyes & Scopes (1991), Lazdunski & Belaich (1972)
15	Adenylate kinase (AK)	V_F	1100	816	0.74	Zikmanis *et al.* (2001)
		K_{mADP}	92	247	2.68	Saint Girons *et al.* (1987)
		K_{eq}	0.5			Goldberg *et al.* (2004)
		K_{mATP}	66	195	2.95	Saint Girons *et al.* (1987)
		K_{mAMP}	38	27	0.71	Saint Girons *et al.* (1987)
16	Ethanol export (ETOHexp)	k	1			Assumed

Table 3. Comparison of the initial steady-state intermediate concentrations derived by ^{31}P NMR studies (Barrow *et al.*, 1984) and model predictions after parameter optimization with specific glucose uptake rate 4.9 g g^{-1} h^{-1} (grams glucose per gram dry weight per hour)

	Concentration (μM)		Ratio
Intermediate	^{31}P NMR	Model	Model/^{31}P NMR
Glucose 6-phosphate	1748	1815	1.04
6-Phosphogluconate	280	268	0.96
6-Phosphogluconolactone		239	
2-Keto-3-deoxy-6-phosphogluconate	630	920	1.46
Glyceraldehyde 3-phosphate	240	354	1.48
1,3-Bisphosphoglycerate		4	
3-Phosphoglycerate	2688	2774	1.03
2-Phosphoglycerate	212	230	1.08
Phosphoenolpyruvate	189	66	0.35
Pyruvate		935	
Acetaldehyde		48	
NAD		1518	
NADH		2982	
ATP*	1500	1671	1.11
ADP*	1500	1313	0.88
AMP*	500	516	1.03

*ATP, ADP and AMP concentrations are assumed according to A(X)P moiety conservation.

Since specific glucose uptake and ATP consumption rates of the cells from which the extracts were obtained were not reported by Algar & Scopes (1985), and our assumed values may slightly differ from those present *in situ*, further model validation was necessary in order to use it for any predictions. Therefore, we undertook a more detailed examination of the optimized model by simulating consumption of 1 M glucose in cell-free extracts reported in the same study (Algar & Scopes, 1985). As in the *in vitro* experiments, we set the initial glucokinase (GK) activity to between 250 and 330 μmol l^{-1} s^{-1} (300 μmol l^{-1} s^{-1}) and proportionally estimated activities for all other enzymes on the basis of previous assumptions and values reported in French-press extracts (Table S2). The total activity of the ADH reaction given by Algar & Scopes (1985) was proportionally distributed between both ADH isoenzymes according to the optimized model. ATP consumption activity was set to that used in the cell-free extracts as externally added enzyme – 200 μmol l^{-1} s^{-1} (Algar & Scopes, 1985). In order to simulate cell-free conditions, both transport reactions were eliminated from the model, and lastly, since initial concentrations for E-D pathway metabolites were not reported by Algar & Scopes (1985), we assumed those according to steady-state concentrations reported for the optimized model (Table 3). Remarkably, the glycolytic flux obtained *in silico* was very similar to that in the *in vitro* experiment (Table 4) and the main difference was the lack of intermediate accumulation which occurred to substantial levels in the experiments. Since metabolite concentrations are much more sensitive to changes in enzyme activity than fluxes, a plausible explanation for the accumulation of intermediates in the *in vitro* experiments might be enzyme denaturation during the time-course resulting in a 'drift' in the steady state, whereas the model simulations assume the enzymes are stable and all remain at their initial levels.

Most importantly, in our *in silico* simulation, the intermediate concentrations obtained were reasonably close to those reported in ^{31}P NMR studies, indicating that computational simulations of the E-D pathway in cell-free extracts reliably simulate the situation *in situ* (Barrow *et al.*, 1984). Therefore, one can speculate that there is no specific 'metabolite tunelling' required for the E-D pathway to proceed, and rather that *Z. mobilis*, in respect to its central glycolytic pathway, can be adequately described as a 'bag of enzymes'.

As demonstrated in other experiments with *Z. mobilis* cell-free extracts, ATPase activity should match closely glucose consumption, and insufficient ATP consumption leads to accumulation of intermediates such as glucose 6-phosphate (Algar & Scopes, 1985). To examine whether this feature can be observed *in silico*, we undertook a series of simulations where, on varying the rate of ATP consumption, we monitored the concentration of glucose 6-phosphate. Indeed, reduction of generalized ATPase activity in the model by 25 % caused accumulation of glucose 6-phosphate to 27 mM and decline of the glycolytic flux by 12 % 60 min after glucose addition. Apart from the fact that this qualitatively resembles the observations in the *in vitro* experiments (Algar & Scopes, 1985), it indicates the control of the glycolytic flux by ATP consumption. To examine this hypothesis in greater detail,

Table 4. Time-course of metabolite levels (in mM) in cell-free extracts after addition of 1.0 M glucose

◆ Data from cell-free experiments by Algar & Scopes (1985); ◇ model simulation. For definitions of intermediates, see Table S1.

		Time (min)						
Intermediate		**0**	**1.5**	**5**	**15**	**30**	**45**	**60**
GLUC	◆		0.98	0.95	0.89	0.75	0.60	**0.48**
	◇	1.00	0.98	0.95	0.86	0.72	0.59	**0.47**
GLUC6P	◆		3.00	2.60	2.80	1.30	0.80	**0.50**
	◇	1.82	4.04	4.64	4.86	3.77	2.55	**1.50**
PGLUCONATE	◆		0.40	0.90	2.00	2.50	1.30	**0.50**
	◇	0.27	0.03	0.03	0.03	0.02	0.02	**0.02**
KDPG	◆		1.30	1.80	3.70	4.80	6.10	**7.00**
	◇	0.92	0.17	0.19	0.21	0.24	0.25	**0.24**
PYR	◆		0.30	0.80	1.00	2.10	7.00	**14.20**
	◇	0.94	0.25	0.24	0.23	0.22	0.21	**0.20**
ACET	◆		0.10	0.80	0.70	1.10	2.00	**3.00**
	◇	0.05	2.07	2.45	3.03	3.56	3.92	**4.20**
ETOH	◆		0.03	0.08	0.23	0.45	0.73	**1.04**
	◇	0.00	0.03	0.10	0.28	0.55	0.82	**1.07**
NAD^+	◆		0.27	0.33	1.00	1.30	1.38	**1.32**
	◇	1.52	3.08	2.75	2.27	1.93	1.73	**1.64**
ATP	◆		0.50	0.10	1.80	2.30	2.00	**1.50**
	◇	1.67	1.91	1.84	1.69	1.50	1.35	**1.19**
Adenylate charge	◆		0.25	0.05	0.69	0.68	0.43	**0.38**
	◇	0.66	0.60	0.59	0.56	0.52	0.49	**0.46**

we carried out a metabolic control analysis investigation using both the initial model and the model simulating glycolysis in cell-free extracts.

Control of glycolytic flux under steady-state conditions

We carried out metabolic control analysis (MCA) for both the optimized model and the model simulating glycolysis in cell-free extracts. The generalized ATP-consuming reaction exerted a major control over glycolytic flux with C_i^J values of 36 and 71 % for the optimized and cell-free extract models, respectively. To extend this finding, we also included in the MCA an optimized model with the activity of the generalized ATP-consuming reaction reduced by 15 % (Table 5). As in the experimental cell-free extracts (Algar & Scopes, 1985), a decrease of generalized ATPase activity resulted in an increase of glucose 6-phosphate steady-state concentration to 16 mM and further reduction of glycolytic flux by almost 10 % (Table 5). In general, the MCA suggested that the ATP-consuming reaction exerts major control over glycolytic flux and, counterintuitively, revealed a negative flux control coefficient for the GK reaction. This result strongly resembles previous experimental observations with *Escherichia coli*, suggesting that the majority of flux control (>75 %) resides not inside but outside the glycolytic pathway, i.e. with the enzymes that hydrolyse ATP (Koebmann *et al.*, 2002). This allowed us to speculate that anabolic reactions, in combination with ATP dissipation by F_0F_1-ATPase, control the glycolytic flux also during the 'uncoupled growth' of *Z. mobilis* when glycolytic flux attains its maximum. [Note that Reyes & Scopes (1991) calculate that F_0F_1-ATPase may contribute over 20 % of the total intracellular ATP turnover.] This is indirectly supported by experiments showing that inhibition of H^+-dependent ATPase results in decline of glycolytic flux and increase of *Z. mobilis* growth yields, suggesting the competition between anabolic and ATP-dissipating reactions (Rutkis and others, unpublished). Flamholz *et al.* (2013) proposed that generally the E-D pathway is favoured by microbes that rely largely on other sources of ATP, so that its lower yield relative to the EMP is insignificant compared with the saving in protein investment in enzymes that they propose arises because of the greater thermodynamic driving force per step. They noted, however, that *Z. mobilis* is an exception as it does not have an additional major source of ATP.

Metabolic control analysis also demonstrates why attempts in the past to increase the glycolytic flux in *Z. mobilis* through overexpression of glycolytic enzymes have been unsuccessful. Negligible flux control coefficients for the majority of the E-D pathway reactions (Table 5) partly explain why overexpression of a few intuitively chosen enzymes has not resulted in the increase of glycolytic flux (Arfman *et al.*, 1992; Snoep *et al.*, 1995). According to MCA, only the pyruvate decarboxylase (PDC) reaction exerts substantial control with C_i^J values reaching 27 % in the optimized model. Based on the flux control coefficients we

Table 5. Scaled flux control coefficients C_i^J of the glycolytic flux in the E-D pathway

Control coefficients above 5 % are shown in bold type.

Reaction	Specific glucose uptake rate (q)		
	4.5*	4.9†	0.197‡
1 GF – glucose facilitator	0	0	–
2 GK – glucokinase	**−8**	**−8**	**−6**
3 GPD – glucose-6-phosphate dehydrogenase	0	1	**7**
4 PGL – 6-phosphogluconolactonase	4	1	3
5 PGD – 6-phosphogluconate dehydratase	3	3	0
6 KDPGA – 2-keto-3-deoxy-6-phosphogluconate aldolase	2	3	0
7 GAPD – glyceraldehyde-3-phosphate dehydrogenase	1	1	0
8 PGK – 3-phosphoglycerate kinase	1	1	0
9 PGM – phosphoglycerate mutase	3	**6**	1
10 ENO – enolase	**11**	**23**	2
11 PYK – pyruvate kinase	2	5	**8**
12 PDC – pyruvate decarboxylase	**11**	**27**	**8**
13 ADH I – alcohol dehydrogenase I	0	0	0
13 ADH II – alcohol dehydrogenase II	0	0	**6**
14 ATPcons – ATP consuming reactions	**70**	**36**	**71**
15 AK – adenylate kinase	0	0	0
16 ETOHexp – ethanol transport	0	0	–

*Optimized model with reduced activity of the generalized ATP-consuming reaction by 15 % – 4400 μmol l^{-1} s^{-1} to 3800 μmol l^{-1} s^{-1}.
†Optimized model.
‡Simulation of the cell-free experiment by Algar & Scopes (1985).

obtain, and earlier reported enzyme activities in recombinant strains (Snoep *et al.*, 1995), we have used equation 5 to calculate the anticipated effects of glyceraldehyde-3-phosphate dehydrogenase (GAPD), 3-phosphoglycerate kinase (PGK), phosphoglycerate mutase (PGM), ADH I, ADH II and PDC overexpression on glycolytic flux in the E-D pathway and compared this to values calculated from experimental data (Table 6). As was observed experimentally, for all enzymes with the exception of PDC, the calculations suggested little or no increase of glycolytic flux in recombinant strains without addition of IPTG, when enzyme activity was increased just a few times. The significantly higher flux control coefficient for the PDC reaction suggested that overexpression of this enzyme more than threefold may lead to an increase of glycolytic flux of almost 23 %. However, such an increase was not observed experimentally; further, experimental observations revealed that a more than 10-fold increase of enzyme activity after addition of 2 mM IPTG slowed down glycolysis by up to 25 %. Given our calculations, this indirectly confirms earlier suggestions that the protein burden effect indeed might be a serious side effect of overexpression of enzymes possessing little or no control over the flux in the E-D pathway. However, in *Z. mobilis*, enzymes involved in fermentation compose as much as 50 % of total protein (Algar & Scopes, 1985), so the protein burden effect might not be as pronounced in other micro-organisms where wild-type levels of E-D pathway enzymes are not so great. Nevertheless, according to equation 3, simultaneous overexpression of PDC, enolase (ENO) and PGM below the protein burden threshold has the potential to increase the glycolytic flux up to 25 % (6.6 g g^{-1} h^{-1}). This clearly demonstrates that the optimized model could serve to develop efficient metabolic engineering strategies for *Z. mobilis* in spite of the protein burden effect. Note also that the EMP pathway (Embden Meyerhof Parnas pathway) could not generate an equivalent glycolytic flux in *Z. mobilis* according to the calculations of Flamholz *et al.* (2013), which suggest that the EMP pathway would need not less than 3.5 times the protein investment for the same flux, which would be infeasible given the 50 % of cell protein already devoted to the E-D pathway.

Co-response analysis and experimental validation

We have recently made measurements of the response of ATP concentration and glycolytic flux to inhibition of ATPase by dicyclohexylcarbodiimide in wild-type *Z. mobilis* and two respiratory chain mutants, *cytB* and *cydB* (Rutkis and others, unpublished). The measurements have been used in neither the construction of the model nor parameter estimation. They allow calculation of the ATP : glycolytic flux co-response coefficient with respect to ATPase using equation 8, as shown in Table S3. The same co-response coefficient can be calculated from the model by simulating it with different levels of ATPase

Table 6. Calculated flux increase values (*f*) for model simulation and experimental data

Reaction	Flux increase value (*f*)			
	Model simulation		Experimental values*	
	0 mM IPTG	2 mM IPTG	0 mM IPTG	2 mM IPTG
GAPD – glyceraldehyde 3-phosphate dehydrogenase	1.006	1.009	0.985	0.748
PGK – 3-phosphoglycerate kinase	1.004	1.009	0.956	0.655
PGM – phosphoglycerate mutase	1.012	1.029	1.005	0.995
PDC – pyruvate decarboxylase	1.229		0.903	
ADH I – alcohol dehydrogenase I	1.000	1.000	0.985	0.767
ADH II – alcohol dehydrogenase II	1.000	1.000	0.981	0.883

*According to Snoep *et al.* (1995).

activity. The experimental and simulated values are shown in Fig. 2, plotted against the glycolytic flux.

The results show that the model correctly captures the relationship between ATP concentration and glycolytic flux for both wild-type and respiratory mutant strains, and also implies that the respiratory deletions have not affected the regulatory pattern of the E-D pathway and catabolic ATP yield per unit of consumed glucose. At the highest glycolytic flux considered (about 4.6 g g^{-1} h^{-1}, ln value 1.53), the co-response coefficient is approximately −4.0. This shows that at this point, ATP homeostasis is poor, since a 1 % increase in glycolytic flux would be associated with a 4 % decrease in ATP concentration. At a flux of about 3.9 g g^{-1} h^{-1}, the co-response coefficient is smaller in magnitude, close to −1.0, where a 1 % increase in glycolytic flux is linked to a 1 % decrease in ATP concentration. At the lowest glycolytic flux obtained with the lowest ATPase activities (3.0 g g^{-1} h^{-1}, ln value 1.1), the co-response coefficient is about −0.23, so that ATP homeostasis is much improved in that it takes a 4 % change in glycolytic flux to produce a 1 % change in ATP concentration in the opposite direction.

CONCLUSIONS

In this study, by using available kinetic parameters, we have developed an *in silico* model of the *Z. mobilis* E-D pathway that also incorporates both ADHs, transport reactions and reactions related to ATP metabolism. Even though parameters of the rate equations were optimized with respect to a single set of conditions, the resulting kinetic model was able to achieve good agreement with previous experimental studies both *in situ* and *in vitro*. The analysis suggests that

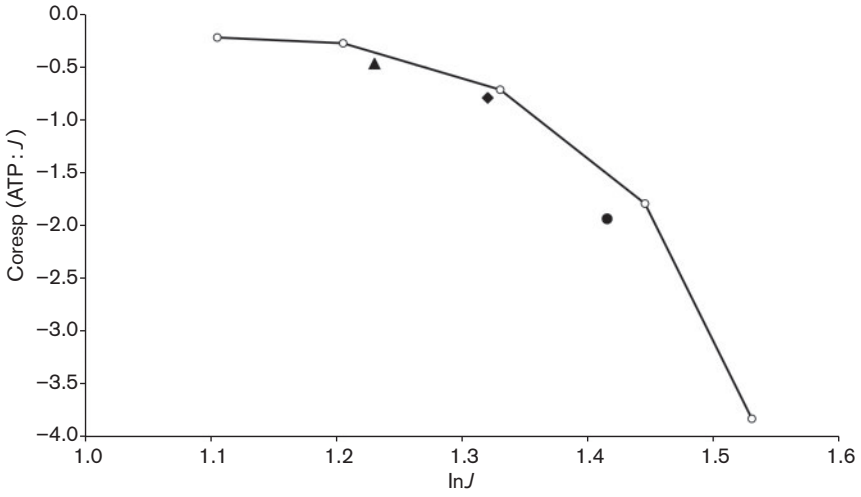

Fig. 2. Experimental and simulated co-response coefficients. ATP and glycolytic flux measurements were made in the absence and presence of 50 μM dicyclohexylcarbodiimide on wild-type and two mutant strains. Co-response coefficients [Coresp (ATP : J)] were calculated as in equation 8. The log of the glycolytic flux (ln*J*) in the uninhibited bacteria averaged 1.5; inhibition of the ATPase lowered the flux and increased the ATP levels. The experimental points are plotted as the mean log value of the flux for the pair of values used for the calculation of the co-response. ◆, Zm6; ●, Zm6-*cytB*; ▲, Zm6-*cydB*; ○, model simulation.

the central glycolytic pathway of *Z. mobilis* can be adequately described as a 'bag of enzymes' and there is no a priori need to invoke 'metabolite channelling' to explain its properties.

MCA analysis revealed that the majority of flux control resides not inside, but outside the E-D pathway. That strongly suggests the need to look for more complex solutions to increasing the glycolytic flux than overexpression of certain E-D pathway enzyme(s). Since the ATP-consuming reactions exerted a major control over the flux in the E-D pathway, their increase, within physiological capacity, making growth more uncoupled, might serve as the appropriate strategy to increase the glycolytic flux in *Z. mobilis*. However, the co-response analysis indicates that cellular ATP homeostasis declines to a critical degree.

On a broader perspective, many other bacteria use the E-D pathway, and this new model may act as a template for simulating their metabolism.

ACKNOWLEDGEMENTS

This work was funded by Latvian European Social Fund projects 2009/027/1DP/1.1.1.2.0/09/APIA/VIAA/128 and 2009/0138/1DP/1.1.2.1.2/09/IPIA/VIAA/004.

REFERENCES

Algar, E. M. & Scopes, R. K. (1985). Studies on cell-free metabolism: ethanol production by extracts of *Zymomonas mobilis*. *J Biotechnol* **2**, 275–287.

Altintas, M. M., Eddy, C. K., Zhang, M., McMillan, J. D. & Kompala, D. S. (2006). Kinetic modeling to optimize pentose fermentation in *Zymomonas mobilis*. *Biotechnol Bioeng* **94**, 273–295.

Atkinson, D. E. (1968). The energy charge of the adenylate pool as a regulatory parameter. Interaction with feedback modifiers. *Biochemistry* **7**, 4030–4034.

Arfman, N., Worrell, V. & Ingram, L. O. (1992). Use of the *tac* promoter and *lacP* for the controlled expression of *Zymomonas mobilis* fermentative genes in *Escherichia coli* and *Zymomonas mobilis*. *J Bacteriol* **174**, 7370–7378.

Barrow, K. D., Collins, J. G., Norton, R. S., Rogers, P. L. & Smith, G. M. (1984). 31P nuclear magnetic resonance studies of the fermentation of glucose to ethanol by *Zymomonas mobilis*. *J Biol Chem* **259**, 5711–5716.

Bisswanger, K. (2002). *Enzyme Kinetics – Principles and Methods*. Weinheim: Wiley.

Bringer-Meyer, S., Schimz, K. L. & Sahm, H. (1986). Pyruvate decarboxylase from *Zymomonas mobilis*: Isolation and partial characterization. *Arch Microbiol* **146**, 105–110.

Cornish-Bowden, A. & Hofmeyr, J.-H. S. (1994). Determination of control coefficients in intact metabolic systems. *Biochem J* **298**, 367–375.

De Graaf, A. A., Striegel, K., Wittig, R. M., Laufer, B., Schmitz, G., Wiechert, W., Sprenger, G. A. & Sahm, H. (1999). Metabolic state of *Zymomonas mobilis* in glucose-, fructose-, and xylose-fed continuous cultures as analysed by 13C- and 31P-NMR spectroscopy. *Arch Microbiol* **171**, 371–385.

Desiniotis, A., Kouvelis, V. N., Davenport, K., Bruce, D., Detter, C., Tapia, R., Han, C., Goodwin, L. A., Woyke, T. & other authors (2012). Complete genome sequence of the ethanol-producing *Zymomonas mobilis* subsp. *mobilis* centrotype ATCC 29191. *J Bacteriol* **194**, 5966–5967.

DiMarco, A. A. & Romano, A. H. (1985). D-Glucose transport system of *Zymomonas mobilis*. *Appl Environ Microbiol* **49**, 151–157.

Doelle, H. W. (1982). Kinetic characteristics and regulatory mechanisms of glucokinase and fructokinase from *Zymomonas mobilis*. *European J Appl Microbiol Biotechnol* **14**, 241–246.

Fell, D. A. (1992). Metabolic control analysis: a survey of its theoretical and experimental development. *Biochem J* **286**, 313–330.

Flamholz, A., Noor, E., Bar-Even, A., Liebermeister, W. & Milo, R. (2013). Glycolytic strategy as a tradeoff between energy yield and protein cost. *Proc Natl Acad Sci U S A* **110**, 10039–10044.

Glaser, L. & Brown, D. H. (1955). Purification and properties of D-glucose-6-phosphate dehydrogenase. *J Biol Chem* **216**, 67–79.

Goldberg, R. N., Tewari, Y. B. & Bhat, T. N. (2004). Thermodynamics of enzyme-catalyzed reactions – a database for quantitative biochemistry. *Bioinformatics* **20**, 2874–2877.

Hofmeyr, J.-H. S., Cornish-Bowden, A. & Rohwer, J. M. (1993). Taking enzyme kinetics out of control; putting control into regulation. *Eur J Biochem* **212**, 833–837.

Hoops, S., Sahle, S., Gauges, R., Lee, C., Pahle, J., Simus, N., Singhal, M., Xu, L., Mendes, P. & Kummer, U. (2006). COPASI – a COmplex PAthway SImulator. *Bioinformatics* **22**, 3067–3074.

Hoppner, T. C. & Doelle, H. W. (1983). Purification and kinetic characteristics of pyruvate decarboxylase and ethanol dehydrogenase from *Zymomonas mobilis* in relation to ethanol production. *Eur J Appl Microbiol Biotechnol* **17**, 152–157.

Jones, C. W. & Doelle, H. W. (1991). Kinetic control of ethanol production by *Zymomonas mobilis*. *Appl Microbiol Biotechnol* **35**, 4–9.

Kacser, H. & Burns, J. A. (1979). Molecular democracy: who shares the controls? *Biochem Soc Trans* **7**(5), 1149–1160.

Kalnenieks, U., De Graaf, A. A., Bringer-Meyer, S. & Sahm, H. (1993). Oxidative phosphorylation in *Zymomonas mobilis*. *Arch Microbiol* **160**, 74–79.

Kalnenieks, U., Galinina, N., Strazdina, I., Kravale, Z., Pickford, J. L., Rutkis, R. & Poole, R. K. (2008). NADH dehydrogenase deficiency results in low respiration rate and improved aerobic growth of *Zymomonas mobilis*. *Microbiology* **154**, 989–994.

Kinoshita, S., Kakizono, T., Kadota, K., Das, K. & Taguchi, H. (1985). Purification of two alcohol dehydrogenases from *Zymomonas mobilis* and their properties. *Appl Microbiol Biotechnol* **22**, 249–254.

Koebmann, B. J., Westerhoff, H. V., Snoep, J. L., Nilsson, D. & Jensen, P. R. (2002). The glycolytic flux in *Escherichia coli* is controlled by the demand for ATP. *J Bacteriol* **184**, 3909–3916.

Kouvelis, V. N., Davenport, K. W., Brettin, T. S., Bruce, D., Detter, C., Han, C. S., Nolan, M., Tapia, R., Damoulaki, A. & other authors (2011). Genome sequence of the ethanol-producing *Zymomonas mobilis* subsp. *pomaceae* lectotype strain ATCC 29192. *J Bacteriol* **193**, 5049–5050.

Kouvelis, V. N., Saunders, E., Brettin, T. S., Bruce, D., Detter, C., Han, C., Typas, M. A. & Pappas, K. M. (2009). Complete genome sequence of the ethanol producer *Zymomonas mobilis* NCIMB 11163. *J Bacteriol* **191**, 7140–7141.

Krietsch, W. K. G. & Bücher, T. (1970). 3-Phosphoglycerate kinase from rabbit skeletal muscle and yeast. *Eur J Biochem* **17**, 568–580.

Lazdunski, A. & Belaich, J. P. (1972). Uncoupling in bacterial growth: ATP pool variation in *Zymomonas mobilis* cells in relation to different uncoupling conditions of growth. *J Gen Microbiol* **70**, 187–197.

Lee, K. J., Skotnicki, M. L., Tribe, D. E. & Rogers, P. L. (1980). Kinetic studies on a highly productive strain of *Zymomonas mobilis*. *Biotechnol Lett* **2**, 339–344.

Neale, A. D., Scopes, R. K., Kelly, J. M. & Wettenhall, R. E. (1986). The two alcohol dehydrogenases of *Zymomonas mobilis*. Purification by differential dye ligand chromatography, molecular characterisation and physiological roles. *Eur J Biochem* **154**, 119–124.

Osman, Y. A., Conway, T., Bonetti, S. J. & Ingram, L. O. (1987). Glycolytic flux in *Zymomonas mobilis*: enzyme and metabolite levels during batch fermentation. *J Bacteriol* **169**, 3726–3736.

Pappas, K. M., Kouvelis, V. N., Saunders, E., Brettin, T. S., Bruce, D., Detter, C., Balakireva, M., Han, C. S., Savvakis, G. & other authors (2011). Genome sequence of the ethanol-producing *Zymomonas mobilis* subsp. *mobilis* lectotype strain ATCC 10988. *J Bacteriol* **193**, 5051–5052.

Parker, C., Peekhaus, N., Zhang, X. & Conway, T. (1997). Kinetics of sugar transport and phosphorylation influence glucose and fructose co-metabolism by *Zymomonas mobilis*. *Appl Environ Microbiol* **63**, 3519–3525.

Pawluk, A., Scopes, R. K. & Griffiths-Smith, K. (1986). Isolation and properties of the glycolytic enzymes from *Zymomonas mobilis*. The five enzymes from glyceraldehyde-3-phosphate dehydrogenase through to pyruvate kinase. *Biochem J* **238**, 275–281.

Pentjuss, A., Odzina, I., Kostromins, A., Fell, D. A., Stalidzans, E. & Kalnenieks, U. (2013). Biotechnological potential of respiring *Zymomonas mobilis*: a stoichiometric analysis of its central metabolism. *J Biotechnol* **165**, 1–10.

Reyes, L. & Scopes, R. K. (1991). Membrane-associated ATPase from *Zymomonas mobilis*; purification and characterization. *Biochim Biophys Acta* **1068**, 174–178.

Robbins, E. A. & Boyer, P. D. (1957). Determination of the equilibrium of the hexokinase reaction and the free energy of hydrolysis of adenosine triphosphate. *J Biol Chem* **224**, 121–135.

Rogers, P. L., Lee, K. J. & Tribe, D. E. (1979). Kinetics of alcohol production by *Zymomonas mobilis* at high sugar concentrations. *Biotechnol Lett* **1**, 165–170.

Rogers, P. L., Lee, K. J., Skotnicki, M. L. & Tribe, D. E. (1982). Ethanol production by *Zymomonas mobilis*. *Adv Biochem Eng* **23**, 37–84.

Rohwer, J. M., Hanekom, A. J., Hendrik, S. & Hofmeyr, J.-H. S. (2007). A universal rate equation for systems biology. *Proceed 2nd Intern ESCEC Symp*, pp. 175–187.

Saint Girons, I., Gilles, A. M., Margarita, D., Michelson, S., Monnot, M., Fermandjian, S., Danchin, A. & Bârzu, O. (1987). Structural and catalytic characteristics of *Escherichia coli* adenylate kinase. *J Biol Chem* **262**, 622–629.

Schoberth, S. M., Chapman, B. E., Kuchel, P. W., Wittig, R. M., Grotendorst, J., Jansen, P. & DeGraff, A. A. (1996). Ethanol transport in *Zymomonas mobilis* measured by using in vivo nuclear magnetic resonance spin transfer. *J Bacteriol* **178**, 1756–1761.

Scopes, R. K. (1983). An iron-activated alcohol dehydrogenase. *FEBS Lett* **156**, 303–306.

Scopes, R. K. (1984). Use of differential dye-ligand chromatography with affinity elution for enzyme purification: 2-keto-3-deoxy-6-phosphogluconate aldolase from *Zymomonas mobilis*. *Anal Biochem* **136**, 525–529.

Scopes, R. K. (1985). 6-Phosphogluconolactonase from *Zymomonas mobilis*. *FEBS Lett* **193**, 185–188.

Scopes, R. K. (1997). Allosteric control of *Zymomonas mobilis* glucose-6-phosphate dehydrogenase by phosphoenolpyruvate. *Biochem J* **326**, 731–735.

Scopes, R. K. & Griffiths-Smith, K. (1984). Use of differential dye-ligand chromatography with affinity elution for enzyme purification: 6-phosphogluconate dehydratase from *Zymomonas mobilis*. *Anal Biochem* **136**, 530–534.

Scopes, R. K. & Griffiths-Smith, K. (1986). Fermentation capabilities of *Zymomonas mobilis* glycolytic enzymes. *Biotechnol Lett* **8**, 653–656.

Scopes, R. K., Testolin, V., Stoter, A., Griffiths-Smith, K. & Algar, E. M. (1985). Simultaneous purification and characterization of glucokinase, fructokinase and glucose-6-phosphate dehydrogenase from *Zymomonas mobilis*. *Biochem J* **228**, 627–634.

Seo, J. S., Chong, H., Park, H. S., Yoon, K. O., Jung, C., Kim, J. J., Hong, J. H., Kim, H., Kim, J. H. & other authors (2005). The genome sequence of the ethanologenic bacterium *Zymomonas mobilis* ZM4. *Nat Biotechnol* **23**, 63–68.

Small, J. R. & Kacser, H. (1993). Responses of metabolic systems to large changes in enzyme activities and effectors. 1. The linear treatment of unbranched chains. *Eur J Biochem* **213**, 613–624.

Snoep, J. L., Yomano, L. P., Westerhoff, H. V. & Ingram, L. O. (1995). Protein burden in *Zymomonas mobilis*: negative flux and growth control due to overproduction of glycolytic enzymes. *Microbiology* **141**, 2329–2337.

Strazdina, I., Kravale, Z., Galinina, N., Rutkis, R., Poole, R. K. & Kalnenieks, U. (2012). Electron transport and oxidative stress in *Zymomonas mobilis* respiratory mutants. *Arch Microbiol* **194**, 461–471.

Strohhäcker, J., De Graaf, A. A., Schoberth, S. M., Wittig, R. M. & Sahm, H. (1993). ^{31}P Nuclear magnetic resonance studies of ethanol inhibition in *Zymomonas mobilis*. *Arch Microbiol* **159**, 484–490.

Swings, J. & De Ley, J. (1977). The biology of *Zymomonas*. *Bacteriol Rev* **41**, 1–46.

Teusink, B., Passarge, J., Reijenga, C. A., Esgalhado, E., van der Weijden, C. C., Schepper, M., Walsh, M. C., Bakker, B. M., van Dam, K. & other authors (2000). Can yeast glycolysis be understood in terms of in vitro kinetics of the constituent enzymes? Testing biochemistry. *Eur J Biochem* **267**, 5313–5329.

Thomas, S. & Fell, D. A. (1996). Design of metabolic control for large flux changes. *J Theor Biol* **182**, 285–298.

Thomas, S. & Fell, D. A. (1998). A control analysis exploration of the role of ATP utilisation in glycolytic-flux control and glycolytic-metabolite-concentration regulation. *Eur J Biochem* **258**, 956–967.

Thomas, T. M. & Scopes, R. K. (1998). The effects of temperature on the kinetics and stability of mesophilic and thermophilic 3-phosphoglycerate kinases. *Biochem J* **330**, 1087–1095.

Vinogradov, A. D. (2000). Steady-state and pre-steady-state kinetics of the mitochondrial F(1)F(0) ATPase: is ATP synthase a reversible molecular machine? *J Exp Biol* **203**, 41–49.

Vogel, G. & Steinhart, R. (1976). ATPase of *Escherichia coli*: purification, dissociation, and reconstitution of the active complex from the isolated subunits. *Biochemistry* **15**, 208–216.

Weisser, P., Krämer, R., Sahm, H. & Sprenger, G. A. (1995). Functional expression of the glucose transporter of *Zymomonas mobilis* leads to restoration of glucose and fructose uptake in *Escherichia coli* mutants and provides evidence for its facilitator action. *J Bacteriol* **177**, 3351–3354.

Wills, C., Kratofil, P., Londo, D. & Martin, T. (1981). Characterization of the two alcohol dehydrogenases of *Zymomonas mobilis*. *Arch Biochem Biophys* **210**, 775–785.

Wold, F. & Ballou, C. E. (1957). Studies on the enzyme enolase. I. Equilibrium studies. *J Biol Chem* **227**, 301–312.

Wurster, B. & Hess, B. (1970). Kinetic analysis of the glucosephosphate isomerase-glucose-6-phosphate dehydrogenase system from yeast *in vitro*. *Hoppe Seylers Z Physiol Chem* **351**, 1537–1544.

Zikmanis, P., Kruce, R. & Auzina, L. (2001). Interrelationships between growth yield, ATPase and adenylate kinase activities in *Zymomonas mobilis*. *Acta Biotechnol* **21**, 171–178.

Edited by: G. Thomas